

Zapozneli lom jekla z visoko trdnostjo

Delayed Fracture of High-strength Steel

B. Ule*, F. Vodopivec*, J. Žvokelj*, M. Grašič* in L. Kosec**

UDK: 669.14.018.2:539.56:620.192.3
ASM/SLA: Q26s, SG Ba, ST, 2—60, EGn, 3—66

V članku so opisane teoretične osnove, potrebne za razumevanje napetostno induciranega segregiranja vodika v jeklu z visoko trdnostjo. Opisano je merjenje kritičnega in mejnega napetostnega intenzitetnega faktorja ter na tej osnovi analiziran vpliv malih mikrostrukturnih variacij jekla na njegovo občutljivost k zapoznemu lomu.

1. UVOD

Ena od znanih oblik porušitve jekla z visoko mejo plastičnosti ter trdnostjo nad 1200 Nmm^{-2} je zapozneli lom, ki nastane zaradi napetostno induciranega segregiranja vodika v jeklu.

Raziskave zapoznelega loma, ki jih je opravil G. L. Hanna s sodelavci¹, kažejo, da obstaja inkubacijski čas do nastanka prve mikrorazpoke; ta počasi raste, vse dokler ne doseže kritične velikosti, kar privede do hipne porušitve. Tako inkubacijski čas, kot tudi čas do loma se podaljšuje z zmanjševanjem obremenitve, vse dokler pri neki dovolj nizki obremenitvi zapozneli lom sploh izostane. A. R. Troiano² je odkril, da nukleacija mikrorazpok izostane tudi v primeru pravočasne razbremenitve, vendar pa se mikrorazpoke pojavi potem, ko je jeklo ponovno daljši čas mehansko obremenjeno. To vodi do sklepa, da je nukleacija mikrorazpok posledica elastične interakcije med mobilnimi atomi vodika v jeklu ter polji troosnih napetosti ob različnih diskontinuitetah kovine.

Lokalno kopičenje vodika v zadostni količini pa poslabša kohezivnost mreže ter olajša nukleacijo mikrorazpok.

2. TEORETIČNI DEL

Atomarni vodik v železu je bodisi na intersticijskih mrežnih mestih, bodisi ujet na različnih napakah kristalne mreže, ki jih imenujemo pasti. Nekaj vodika najdemo vedno tudi v molekularni obliki v porah.

Koncept pasti sta predlagala Darken in Smith³, da bi pojasnila vpliv temperature in koncentracije vodika v železu na njegovo difuzivnost. Oriani⁴ je kasneje na osnovi različnih eksperimentalnih podatkov izračunal vezavno energijo, s katero je vodik vezan v pasteh. Skoraj v vseh primerih je dobil vrednosti okrog 27 kJ na mol vodika. Podobne vrednosti so navedene tudi v referencah 5,6 in 7, čeprav sta Kumnick in Johnson⁵ odkrila tudi pasti z vezavno energijo približno 60 kJ na mol vodika. Gostoto teh pasti, vejetno so bili to dislokacijski pragovi, sta ocenila na 10^{23} m^{-3} v močno deformiranem železu.

Danes je znano, da kot pasti delujejo skoraj vse nepravilnosti kristalne mreže kovin, tako dislokacije^{9,10},

The paper presents theoretical fundamentals to understand the stress-induced hydrogen segregation in high-strength steel.

Measurements of the critical and of the threshold stress intensity factor are presented which represent the basis for analysing the influence of small microstructural variations of steel on its sensitivity to the delayed fracture.

1. INTRODUCTION

Delayed fracture caused by stress-induced hydrogen segregation is one of the known types of failure of steel with high yield strength and tensile strength above 1200 N mm^{-2} .

Investigations of the delayed fracture by G. L. Hanna and coworkers¹ showed an incubation period before the nucleation of the first microcrack, a slow growth of the microcrack and an instantaneous failure when a critical size was reached. The incubation period as well as the time till failure occurs are prolonged with the decreased load until at a sufficiently low load the delayed fracture does not occur at all.

A. R. Troiano² found that nucleation of microcracks does not appear if the unloading took place in the due time, but microcracks occur after steel was again mechanically loaded for a longer time. This leads to the conclusion that the nucleation of microcracks is a consequence of elastic interaction between the mobile hydrogen atoms in steel and the triaxial stress fields at different discontinuities in the metal. Local accumulations of hydrogen at a sufficient level diminish the cohesive forces in the lattice and facilitate the nucleation of cracks.

2. THEORY

Atomic hydrogen in iron is found either in interstitial sites of the lattice or it is as trapped hydrogen bound on different imperfections of the crystal lattice, being called "traps". Some hydrogen in molecular form is found always in the microvoids too.

Darken and Smith³ suggested the concept of traps to explain the influence of temperature and of concentration on the diffusivity of hydrogen in iron. Later, on basis of experimental data, Oriani⁴ calculated the trap binding energy of hydrogen and obtained value of about 27 kJ/mole hydrogen in almost all the cases. Similar values are quoted also in refs. 5, 6 and 7, while Kumnick and Johnson⁵ discovered traps with the binding energy of about 60 kJ/mole hydrogen too. The density of traps, probably dislocation jogs, were estimated to 10^{23} m^{-3} in a heavily deformed iron.

* Metalurški inštitut, Lepi pot 11, Ljubljana

** Univerza Edvarda Kardelja, FNT — Montanistika, Aškerčeva 20, Ljubljana

pore^{11, 12}, meje zrn¹³, mejne površine kovina-karbidi delci¹⁴, kot tudi površine nekovinskih vključkov^{15, 16}.

Matematični model za opis vodika v pasteh sta razvila Foster in McNabb¹⁷. Po njunem modelu je v pasteh ujeti vodik v lokalnem ravnotežu z interstičijskim vodikom. Interakcija med vodikom in pastmi je termično aktiviran proces z aktivacijsko energijo, ki jo sestavljata vezavna energija pasti ter aktivacijska energija za difuzijo vodika v idealni mreži železa, ki dosega vrednost 12 kJ na mol vodika.

Gonila sila za interstičijsko difuzijo raztopljenega vodika v kovinah je gradient kemičnega potenciala vodika. K temu gradientu prispevajo koncentracijske razlike ter učinki polj elastičnih napetosti. Termodynamični učinek polj elastičnih napetosti je utemeljen z reverzibilno dilatacijo kristalne mreže kovin ter pozitivno spremembo volumna, ki spremi vgnezdjenje vodikovih intersticij v področja pozitivne deformacije, medtem, ko se področja s tlačno deformacijo z vodikom osirošajo. Na ta način je z nehomogeno prerazporeditvijo vodika dosežen krajevno neodvisen kemični potencial vodika v nehomogenem polju elastičnih napetosti.

Li, Oriani in Darken¹⁹ so s termodynamično analizo problema, pri čemer so vodik v železu obravnavali kot povsem mobilno komponento, izpeljali naslednjo enačbo:

$$\mu_H = \mu_H^0 + RT \ln[H] - \sigma_h \bar{V}_H \quad (1)$$

v kateri prva dva člena določata kemični potencial vodika v odvisnosti od njegove koncentracije, \bar{V}_H je fenomenološki parcialni atomski volumen vodika v železu, σ_h pa je hidrostatična komponenta napetostnega tenzorja, s katerim popišemo troosno napetostno stanje. Ob predpostavki, da je v ravnotežju kemični potencial vodika krajevno neodvisen, z enačbo (1) izračunamo koncentracijo vodika v področju maksimalne hidrostatične komponente napetostnega tenzorja v razdalji r pred korenem zareze:

$$[H]_r = [H] \exp(\sigma_h \bar{V}_H / RT), \quad (2)$$

kjer je $[H]$ povprečna koncentracija vodika v preizkušnici.

Za ravninsko deformacijsko stanje, način obremenitve I ter za ravnino napredovanja razpok iz korena zareze uporabimo naslednjo enačbo²⁰:

$$\sigma_h = 2(1+v) K_I / 3\sqrt{2\pi r} \quad (3)$$

Iz enačb (2) in (3) dobimo:

$$[H]_r = [H] \exp \frac{2(1+v) K_I \bar{V}_H}{3RT\sqrt{2\pi r}} \quad (4)$$

Enačba (4) povezuje napetostni intenzitetni faktor K_I ter koncentracijo vodika v razdalji r pred korenem zareze.

Dejstvo, da pri apliciranem napetostnem intenzitetnem faktorju K_I , ki je nižji od mejnega napetostnega intenzitetnega faktorja K_{TH} zapozneli lom sploh izostane, je Beachem²¹ zapisal v obliki kriterija, ki določa pogoje pojavljanja tega loma:

$$K_{TH} < K_I < K_{Ic} \quad (5)$$

kjer je K_{Ic} kritični napetostni intenzitetni faktor.

Gerberich²² je na osnovi bodisi mehanizma Troiano-Oriani^{2, 23} bodisi Beachemove hipoteze²⁴ postuliral kritično koncentracijo vodika $[H]_r^{cr}$, ki v razdalji r pred korenem zareze povzroči nukleacijo mikrorazpok. Predpostavil je, da je kritična koncentracija vodika lahko dosežena le, ako deluoča mehanska obremenitev preseže neko mejno vrednost, kar lahko zapišemo kot:

$$K_I \geq K_{TH} \Rightarrow [H]_r = [H]_r^{cr} \quad (6)$$

At present, it is known that almost all the kinds of imperfections in the crystal lattice of metals, both dislocations^{9, 10}, microvoids^{11, 12}, grain boundaries¹³, metal-carbide interfaces¹⁴, and the surfaces of non-metallic inclusions^{15, 16} can act as trapping sites.

A mathematical model of hydrogen traps was developed by Foster and McNabb¹⁷. According to the model, trapped hydrogen is locally in equilibrium with the interstitial hydrogen. The interaction between hydrogen and the traps is a thermally activated process with an activation energy constituted of the binding trap energy, and the activation energy of diffusion of hydrogen in an ideal iron lattice being 12 kJ/mole hydrogen¹⁸.

The driving force for the interstitial diffusion of the dissolved hydrogen in metals is the gradient of chemical potential. This gradient is influenced by the differences in hydrogen concentrations and by the effects of elastic-stress fields. The thermodynamic effect of the elastic-stress fields is caused by the reversible dilatation of the crystal lattice of metals, and the positive volume change accompanied by the insertion of hydrogen interstitials into the areas of positive strain, while compressively strained regions are impoverished with hydrogen. Thus a locally independent chemical potential of hydrogen in an inhomogeneous elastic-stress field is obtained through an inhomogeneous redistribution of hydrogen.

The thermodynamic analysis of this process, under supposition that hydrogen is a completely mobile component, was established by Li, Oriani and Darken¹⁹ who developed the following equation:

$$\mu_H = \mu_H^0 + RT \ln[H] - \sigma_h \bar{V}_H \quad (1)$$

The first two terms determine the chemical potential of hydrogen depending on its concentration, \bar{V}_H is the phenomenological partial atomic volume of hydrogen in iron, while σ_h is the hydrostatic component of the stress tensor describing the triaxial state of stresses. Supposing that the chemical potential of hydrogen in equilibrium is locally independent, the concentration of hydrogen in the region of the maximal hydrostatic component of stress tensor is given at a distance r from the notch root by (1):

$$[H]_r = [H] \exp(\sigma_h \bar{V}_H / RT), \quad (2)$$

with $[H]$ as an average concentration of hydrogen in the specimen.

For a plane strain state, for a mode of loading I, and for the plane crack propagation from the notch root, the following equation is given²⁰:

$$\sigma_h = 2(1+v) K_I / 3\sqrt{2\pi r} \quad (3)$$

From equations (2) and (3) we obtain:

$$[H]_r = [H] \exp \frac{2(1+v) K_I \bar{V}_H}{3RT\sqrt{2\pi r}} \quad (4)$$

The equation (4) connects the stress intensity factor K_I with the concentration of hydrogen at the distance r from the notch root. The fact, that the delayed fracture does not occur if the applied stress intensity factor K_I is lower than the threshold stress intensity factor K_{TH} , has been applied by Beachem²¹ as the criterion to determine the conditions under which the delayed fracture takes place:

$$K_{TH} < K_I < K_{Ic}, \quad (5)$$

where K_{Ic} is the critical stress intensity factor.

On the basis of the Troiano-Oriani mechanism^{2, 23} or the Beachem hypothesis²⁴, the critical concentration of

S kombiniranjem enačb (4) in (6) dobimo:

$$K_{TH} = \frac{3 RT / 2\pi r}{2(1+v) \bar{V}_H} \ln \left\{ \frac{[H]_r^{cr}}{[H]} \right\} \quad (7)$$

Enačba (7) velja le v primeru, ko je plastična zona ob konici zareze omejena na manj kot eno kristalno zrno velikosti d. Če upoštevamo, da je vpletten še vodik, ujet na mejah zrn, lahko pišemo:

$$K_{TH} = \frac{3 RT / 2\pi d}{2(1+v) \bar{V}_H} \ln \left\{ \frac{[H]_r^{cr}}{[H]} \right\}; d \geq R_i, \quad (8)$$

kjer je R_i velikost plastične cone pri ravnninskem deformacijskem stanju ter načinu obremenitve I.

Z izrazom (8) ni mogoče pojasnit eksperimentalno ugotovljene odvisnosti med K_{TH} ter mejo plastičnosti.

Upoštevaje še vpliv polja drsnih linij ob korenju zareze, dobimo po Gerberichu²² za K_{TH} naslednji izraz:

$$K_{TH} = \frac{RT}{\alpha \bar{V}_H} \ln \left\{ \frac{[H]_r^{cr}}{[H]} \right\} - \frac{\sigma_{ys}}{2\alpha} \quad (9)$$

Omeniti je potrebno, da pri meji plastičnosti pod 1200 N/mm⁻² pogosto prihaja do neujemanja med enačbo (9) ter rezultati eksperimentov. Deloma lahko to neujemanje razložimo z odvisnostjo razmerja $[H]^{cr}/[H]$ od meje plastičnosti jekla. Farrell in Quarrell²³ sta namerič ugotovila, da so za doseganje krhkosti v jeklih z nižjo mejo plastičnosti potrebne višje koncentracije vodika, kar sta zapisala kot $[H]^{cr} \propto 1/\sigma_{ys}$. Kim in Loginow²⁷ pa sta pokazala, da se v jeklih z višjo mejo plastičnosti topi več vodika, torej $[H] \propto \sigma_{ys}$. Končno dobimo:

$$\frac{[H]^{cr}}{[H]} = \frac{\beta}{\sigma_{ys}}, \quad (10)$$

pri čemer je β konstanta za posamično vrsto jekla.

3. EKSPERIMENTALNI DEL Z REZULTATI

3.1 Izberi jekla in geometrija preizkušancev

Cilj preiskave je bila ugotovitev vpliva mikrostrukturnih variacij visokotrdnega jekla z 0,40 % C, 0,31 % Si, 0,71 % Mn, 0,019 % P, 0,006 % S, 1,03 % Cr, 0,21 % Mo, 0,26 % Cu, 0,009 % Al in 0,010 % Sn na občutljivost k z vodikom induciranimu pokanju. Jeklo je bilo izdelano po VOD postopku, zato vsebuje le malo žvepla, analize pa so pokazale, da vsebnost residualnega vodika ne presega 0,05 ppm. Navezni preizkusi so bili opravljeni s preizkušanci z zarezo, katerih geometrija je prikazana na sliki 1. Po podatkih iz literature²⁷ je za takšne preizkušance odvisnost med napetostnim intenzitetnim faktorjem K_i , njih geometrijo ter aksialno delujejočo silo P dana z izrazom:

$$K_i = \frac{P}{D^{3/2}} (-1,27 + 1,72 D/d) \quad (11)$$

pri pogoju:

$$0,5 < d/D < 0,8$$

Razmerje P/D , pri čemer je P korenski radius zareze, je bilo blizu vrednosti 0,02. Moran in Noris²⁹ sta z računalniško simulacijo nateznega preizkusa cilindričnih preizkušancev z zarezo po obodu ugotovila, da se pri razmerju $P/D = 0,01$ do $0,02$ pojavljajo maksimalne napetosti ob lomu preizkušanca za približno dva korenska radiusa pod površino, medtem ko so maksimalne defor-

hydrogen $[H]_r^{cr}$ which produces crack nucleation at the distance r from the notch root was postulated by Gerberich²². He assumed that the critical concentration of hydrogen could be achieved only if the applied load exceeds a certain limiting value, which could be written as:

$$K_i \geq K_{TH} \Rightarrow [H]_r = [H]_r^{cr} \quad (6)$$

Combining Eqs. (4) and (6) we obtain:

$$K_{TH} = \frac{3 RT / 2\pi r}{2(1+v) \bar{V}_H} \ln \left\{ \frac{[H]_r^{cr}}{[H]} \right\} \quad (7)$$

The equation (7) is correct only when the plastic zone at the notch tip is limited to less than the grain diameter d . Considering that also hydrogen on the grain boundaries at the crack tip is involved, we can write:

$$K_{TH} = \frac{3 RT / 2\pi d}{2(1+v) \bar{V}_H} \ln \left\{ \frac{[H]_r^{cr}}{[H]} \right\}; d \geq R_i, \quad (8)$$

with R_i as the size of the strain plastic zone under mode of loading I.

On the basis of equation (8) it is not possible to explain the connection between the yield strength effect and K_{TH} , though it has been established by experiments.

If taking into account the influence of a slip-line field at the notch root, according to Gerberich²², we obtain for K_{TH} :

$$K_{TH} = \frac{RT}{\alpha \bar{V}_H} \ln \left\{ \frac{[H]_r^{cr}}{[H]} \right\} - \frac{\sigma_{ys}}{2\alpha} \quad (9)$$

It is necessary to mention that disagreements are often observed between Eq. (9) and experimental results at yield strength below 1200 N/mm⁻². These disagreements were explained partly by the dependence of the $[H]^{cr}/[H]$ ratio on the yield point. Namely Farrell and Quarrell²³ ascertained that larger concentrations of hydrogen are needed to produce embrittlement in steel with lower yield strength, and postulated the relationship $[H]^{cr} \propto 1/\sigma_{ys}$.

Kim and Loginow²⁶ suggested that the content of soluble hydrogen in steel was proportional to the yield strength, therefore $[H] \propto \sigma_{ys}$. Finally, we obtain:

$$\frac{[H]^{cr}}{[H]} = \frac{\beta}{\sigma_{ys}}, \quad (10)$$

with β as constant for a single type of steel.

3. EXPERIMENTS AND RESULTS

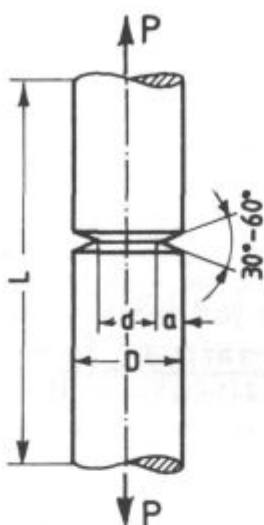
3.1 Selection of Steel and the Geometry of Specimens

The aim of the investigation was to establish the influence of microstructure on the hydrogen induced susceptibility to cracking of a high-strength steel with the composition: 0.40 % C, 0.31 % Si, 0.71 % Mn, 0.019 % P, 0.006 % S, 1.03 % Cr, 0.21 % Mo, 0.26 % Cu, 0.009 % Al and 0.010 % Sn. The steel was manufactured by the VOD process, thus the content of sulphur was low and the concentration of residual hydrogen did not exceed 0.05 ppm.

Tensile tests were made on notched tensile specimens with the geometry shown in Fig. 1. For these specimens, the relationship between the stress intensity factor K_i , the geometry, and the axial force P is given by the equation²⁷:

$$K_i = \frac{P}{D^{3/2}} (-1,27 + 1,72 D/d) \quad (11)$$

macije dosežene v samem korenju zareze, kjer se sicer pojavljajo prve mikrorazpoke.



Slika 1

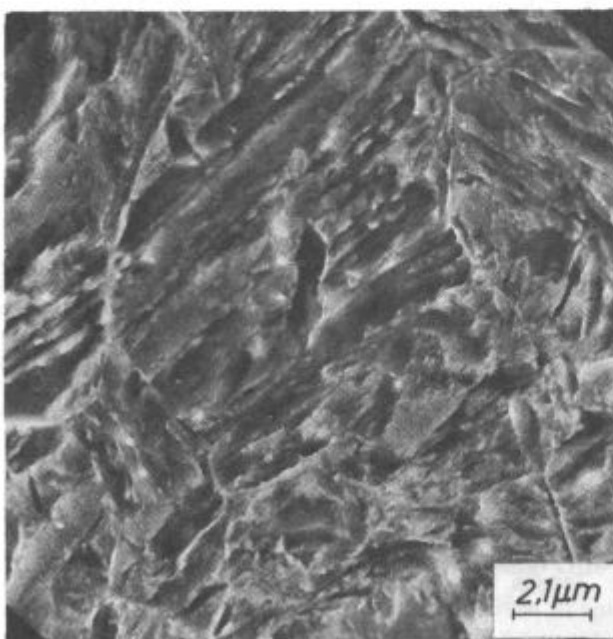
Geometrija cilindričnih nateznih preiskušancev z zarezo po obodu.

Fig. 1

Geometry of cylindrical round notched tensile specimens.

3.2 Toplotna obdelava

Toplotna obdelava preizkušancev je obsegala 1/2-urno avsténitizacijo pri 850°C s kaljenjem v vodi oziroma olju ter popuščanje. Slika 2 prikazuje mikrostrukturo letvastega martenzita, izoblikovanega pri kaljenju v vodi. S popuščanjem 2 ur pri 480°C oziroma 420°C je bila dosežena meja plastičnosti 1185 oziroma 1290 Nmm^{-2} .



Slika 2

Avsténitizirano pri 850°C in kaljeno v vodi. Letvasti martenzit.

Fig. 2

Austenitized at 850°C , and quenched in water. Lath-shaped martensite.

under condition that:

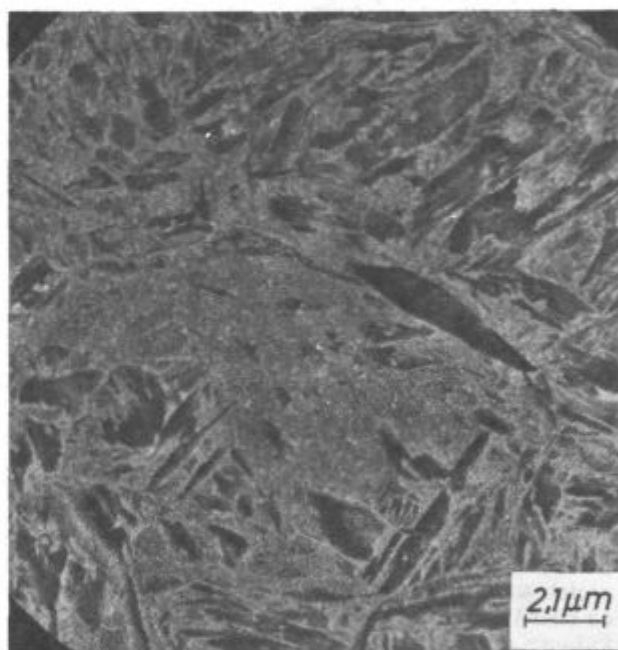
$$0.5 < d/D < 0.8$$

The ratio p/D , with p as the notch root radius, was close to the value 0.02. Moran and Noris²⁸ found by the computer simulation of the tension test with cylindrical, peripherally notched specimens, that the maximum stresses at fracture occur at about two notch-root radii below the surface when the p/D ratio is 0.01 to 0.02. On the other hand the maximum strain occurs at the notch root where also the first microcracks appear.

3.2 Thermal Treatment

Thermal treatment of specimens consisted of a 30 mins. austenitisation at 850°C , quenching in water or in oil, and tempering.

Fig. 2 shows the microstructure of the lath-formed martensite in the steel quenched in water. After tempering 2 hrs. at 480°C or 420°C yield strengths of 1185 and 1290 N mm^{-2} respectively were obtained. The hardness of oil quenched specimens was between 52 and 53.7 HRC. This means, that the predominantly martensitic microstructure of oil quenched specimens (Fig. 3) still contains up to 3 % of bainite. After tempering specimens quenched in oil 2 hrs. at 450°C , a yield strength of 1230 N mm^{-2} was obtained.



Slika 3

Avsténitizirano pri 850°C in kaljeno v olju. Spodnji bainit v martensiti osnovi.

Fig. 3

Austenitized at 850°C , and quenched in oil. Lower bainite in the martensitic matrix.

3.3 Hydrogen Charging

After thermal treatment, the specimens were charged with hydrogen by etching 24 hrs. in a 0.1 N aqueous solution of hydrochloric acid.

Chemical analysis of specimens immediately after the removal from the acid solution showed a hydrogen concentration of $2.9 \pm 0.1 \text{ ppm}$ independently upon the yield

Trdota v olju kaljenih preizkušancev je dosegala vrednosti med 52 in 53,7 HRc. Pomeni, da je v pretežno martenzitni mikrostrukturi tovrstnih preizkušancev po kaljenju v olju (sl. 3) še tudi do 3 % bainita. S popuščanjem v olju kaljenih preizkušancev 2 ur pri 450°C je bila dosegrena meja plastičnosti 1230 Nmm⁻².

3.3 Navodičenje

Toplotni obdelavi je sledilo navodičenje preizkušancev z jedkanjem 24 ur v 0,1 N vodni raztopini solne kisline.

Kemične analize vzorcev neposredno po odstranitvi iz kisline kažejo, da dobljena koncentracija vodika 2,9±0,1 ppm praktično ni odvisna od meje plastičnosti jekla. Z drugimi besedami: s 24-urnim jedkanjem še ni dosegena stacionarna koncentracija nasičenja jekla z vodikom. Zaključujemo, da del pasti še ni zaseden, saj bi v takšnem primeru bila koncentracija vodika različna v preizkušancih z različno mejo plastičnosti^{26, 29}.

24 ur po odstranitvi iz raztopine je koncentracija vodika v preizkušancih padla na 0,82±0,1 ppm ter 48 ur po odstranitvi na 0,58±0,08 ppm.

Ob predpostavki, da je hitrost uhajanja vodika iz cilindričnih preizkušancev majhnega premera (D je približno 7 mm) premo sorazmerna razlike med trenutno ter residualno koncentracijo vodika v njih, dobimo za koncentracijo vodika v odvisnosti od časa po jedkanju (v urah) naslednji izraz:

$$[H] = 0,55 + 2,35 \exp(-0,09 t) \quad (12)$$

Polempiričen izraz (12) je uporaben za fenomenološki opis uhajanja vodika iz cilindričnih preizkušancev in ugotovljeno je bilo³⁰, da v navodičenih preizkušancih ostaja še okrog 0,55 ppm vodika tudi dolgo časa po končanem jedkanju.

3.4 Določevanje kritičnega ter mejnega napetostnega intenzitetnega faktorja

Razvit je bil eksperimentalni sklop za registriranje inkubacijskega časa, to je časa do porajanja prve mikrorazpoke ter za registriranje počasnega napredovanja mikrorazpok do hipnega loma statično obremenjenih preizkušancev z zarezo po obodu. Sestavljen je bil iz polovičnega Wheatstonevega mostička z variabilnim uporom, ki ga je predstavljal uporovni listič, nalepljen preko ustja zareze. Porajanje ter napredovanje mikrorazpok je bilo registrirano posredno z odpiranjem ustja zareze, kot spremembra upornosti aktivnega uporovnega

strength of steel. In the other words, a 24 hrs. etching did not produce the saturation of steel with hydrogen. It was concluded that all the traps were not filled since in such a case the concentration of hydrogen in steel would be different in samples with different yield strengths^{26, 29}. Twenty-four hours after removal from the acid solution, the concentration of hydrogen in specimens dropped to 0.82±0.1 ppm and after 48 hours to 0.58±0.08 ppm.

Supposing that the escape rate of hydrogen from the cylindric specimens with small diameter (D is approx. 7 mm) is proportional to the difference between the actual and the residual hydrogen concentration, the following equation can be derived for the variation of hydrogen concentration with time (hours) after the removal of samples from the acid solution:

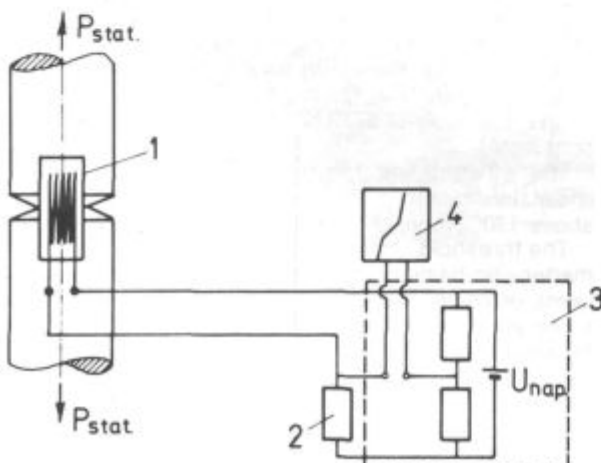
$$[H] = 0,55 + 2,35 \exp(-0,09 t) \quad (12)$$

This semiempirical equation is useful for the phenomenological description of hydrogen losses from the cylindric specimens and as it has been established³⁰ that the specimens charged with hydrogen still contain residual hydrogen of about 0.55 ppm even a long time after the etching.

3.4 Determination of the Critical and the Threshold Stress Intensity Factor

An experimental set-up was developed for the registration of the incubation period i.e. of the time necessary for the nucleation of the first microcrack, as well as for the registration of the slow propagation of microcracks to the instantaneous fracture of the round-notched specimens under static load. It consisted of a half-Wheatston bridge with a variable resistor represented by a strain-gauge stucked across the notch opening. Nucleation of microcracks and their propagation were indirectly registered by the displacement of the notch opening as the change of the resistance of the active strain-gauge compared with the resistance of the reference strain-gauge. This experimental set-up (schematically shown in Fig. (4)) permitted to detect the propagation steps of about 0.1 μm.

An almost similar set-up was used to measure the critical stress intensity factor i.e. fracture toughness of steel. Fig. 5 shows how the measurements were made on the "Instron" tensile machine with an accurate extensometer mounted on the notch opening of the specimen for calibration of the strain-gauges.



Slika 4

Eksperimentalni sklop za zasledovanje porajanja ter napredovanja mikrorazpok (1 — natezni preiskušec z uporovnim lističem, 2 — referenčni uporovni listič, 3 — merilna enota z izvorom napetosti, galvanometrom ter ojačevalcem, 4 — registrator).

Fig. 4

Experimental set-up for the detection of crack nucleation and propagation (1 — tensile specimen with strain-gauge, 2 — reference strain-gauge, 3 — measuring unit with power source, galvanometer and amplifier, 4 — recorder).



Slika 5

Merjenje lomne žilavosti. Ekstenzometer na preiskušanju služi kalibriraju uporavnih lističev.

Fig. 5

Measurement of fracture toughness. Extensometer on the tensile specimen used for the calibration of the strain-gauges.

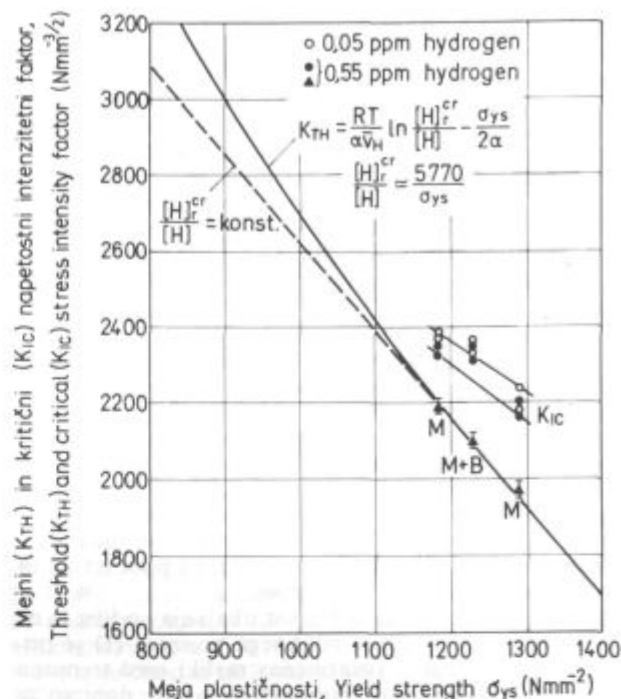
lističa glede na upornost referenčnega uporavnega lističa. Eksperimentalni sklop (shematsko prikazan na sliki 4) je dovoljeval zaznavanje koraka propagacije okrog 0,1 μm.

Skoraj podoben sklop opreme je bil uporabljen za merjenje kritičnega napetostnega intenzitetnega faktorja, t. j. lomne žilavosti jekla. Na sliki 5 je prikazana izvedba merjenja na trgalnem stroju »Instron« s preciznim ekstenzometrom, montiranim preko ustja zareze preizkušanca ter uporabljenim za kalibriranje uporavnih lističev.

Z merjenjem časa do loma preizkušancev v odvisnosti od uporabljene obremenitve je bil eksperimentalno določen mejni napetostni intenzitetni faktor K_{TH} , to je mejna statična obremenitev, pri kateri še ne pride do nukleacije mikrorazpok.

Kritični napetostni-intenzitetni faktor K_{Ic} , t. j. lomna žilavost jekla je bila izmerjena na cilindričnih preizkušancih z zarezo ter utrujenostno razpoko v korenju zareze. Tako kot za izračun mejnega, je bila tudi za izračun kritičnega napetostnega intenzitetnega faktorja uporabljena formula (11), globina utrujenostne propagacije mikrorazpok pa je bila izmerjena z optičnim mikroskopom po vsakokratnem preizkuusu.

Za preverjanje rezultatov je bila lomna žilavost izračunana še s korelacijo Rolfe-Novak³¹ za takoimenovano upper shelf področje. Odvisnost med izmerjenimi faktorji (K_{TH} , K_{Ic}) ter mejo plastičnosti jekla je prikazana



Slika 6

Odvisnost med napetostnim intenzitetnim faktorjem (K_{TH} , K_{Ic}) in mejo plastičnosti preiskovanega jekla.

Fig. 6

Relationship between the stress intensity factor (K_{TH} , K_{Ic}) and the yield strength of the investigated steel.

The threshold stress intensity factor K_{TH} which represents the limiting value of static load below which micro-cracks do not appear, was experimentally determined by measuring the time till fracture occurs related to the applied load.

The critical stress intensity factor K_{Ic} i. e. the fracture toughness of steel was measured on round notched tensile specimens with fatigue crack at the notch tip. The Eq. (11) was applied to calculate both the threshold and the critical stress intensity factor. The width of the fatigue crack was measured with an optical microscope after each experiment.

To check the obtained results, the fracture toughness was also calculated by the Rolfe-Novak correlation³¹ for the upper shelf region. The relation between the measured factors (K_{TH} , K_{Ic}) and the yield strength of the investigated steel is shown in Fig. 6. The plot presents also the relation by eq. (9) calculated on the basis of measured values for steel with fully martensitic microstructure after quenching (points M). Considering the equation (10), a value of 5770 N mm⁻² was calculated for the constant β.

The straight line for $[H]_{cr}^{cr}/[H] = \text{const.}$ proves that linear interpolation is acceptable at yield strengths above 1200 N mm⁻².

The threshold stress intensity factor K_{TH} for tempered martensitic-bainitic microstructure with only few percents of bainite after quenching (point M+B) has the same value as that for a fully martensitic tempered microstructure with the same yield strength ($K_{TH} = 2100$ N mm^{-3/2}).

Hydrogen has no noticeable influence, if any at all, on the fracture toughness of the investigated steel. However, at the same yield strength, the fracture toughness,

na sliki 6. V diagramu je vrisana tudi odvisnost (9), izračunana na osnovi izmerjenih vrednosti za jeklo s povsem martenzitno mikrostrukturo po kaljenju (točki M). Upoštevaje izraz (10) ima konstanta β vrednost 5770 Nmm^{-2} .

Premica za $[H]^{cr}/[H] = \text{konst.}$ dokazuje, da je pri meji plastičnosti nad 1200 Nmm^{-2} dopustna linearna interpolacija.

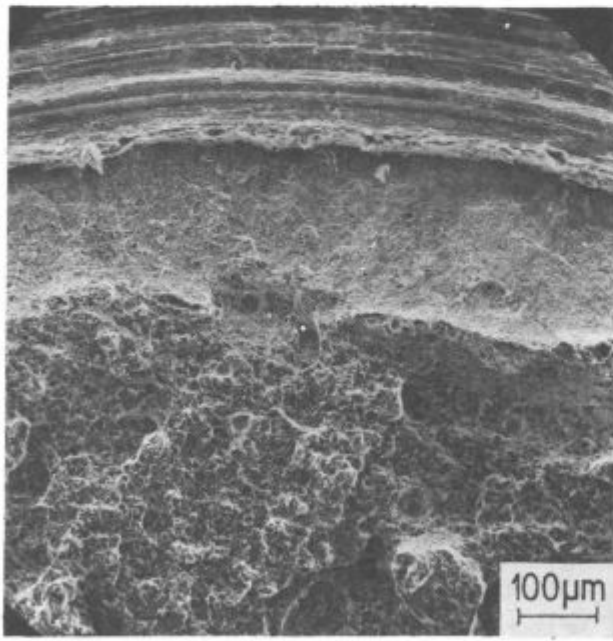
Mejni napetostni intenzitetni faktor K_{TH} za popuščeno martenzitno-bainitno mikrostrukturo z le nekaj odstotki bainita po kaljenju (točka M+B) ima enako vrednost, kot je bila določena za jeklo z mikrostrukturo popuščenega martenzita ter enako mejo plastičnosti ($K_{TH} = 2100 \text{ Nmm}^{-3/2}$).

Vodik nima večjega, če ima sploh kakšen vpliv na lomno žilavost preiskovanega jekla. Pri enaki meji plastičnosti pa je lomna žilavost, v nasprotju z mejnim napetostnim intenzitetnim faktorjem, nekoliko odvisna od majhnih mikrostrukturnih variacij jekla. Tako ima jeklo s popuščeno martenzitno-bainitno mikrostrukturo ter mejo plastičnosti 1230 Nmm^{-2} lomno žilavost med 2310 in $2360 \text{ Nmm}^{-3/2}$, kar je nekoliko več od z linearno interpolacijo določene lomne žilavosti za popuščeno martenzitno mikrostrukturo enake meje plastičnosti ($K_{lc} = 2250$ in $2320 \text{ Nmm}^{-3/2}$).

3.5 Mikromorfologija prelomov

Mikrofraktografske preiskave prelomnih površin navodičenih cilindričnih nateznih preizkušancev z zarezo po obodu, so bile opravljene z vrstičnim elektronskim mikroskopom.

Slika 7 kaže del prelomne površine nateznega preizkušanca z zarezo, z mikrostrukturo popuščenega martenzita ter mejo plastičnosti 1185 Nmm^{-2} . Statična



Slika 7

Z zapoznanim lomom nastala prelomna površina preizkušanca z mikrostrukturo popuščenega martenzita ter mejo plastičnosti 1185 N mm^{-2} posneta z vrstičnim elektronskim mikroskopom.

Fig. 7

Scanning electron micrographs of the delayed fracture surfaces of specimen with the tempered martensitic microstructure and yield strength 1185 N mm^{-2} .

contrary to the threshold stress intensity factor, depends slightly on small microstructure variations of steel. For instance, steel with the martensitic-bainitic microstructure with yield strength 1230 N mm^{-2} has fracture toughness between 2310 and $2360 \text{ N mm}^{-3/2}$, which is slightly above the value of K_{lc} being between 2250 and $2320 \text{ N mm}^{-3/2}$ found by linear interpolation for the tempered martensitic microstructure with the same yield strength.

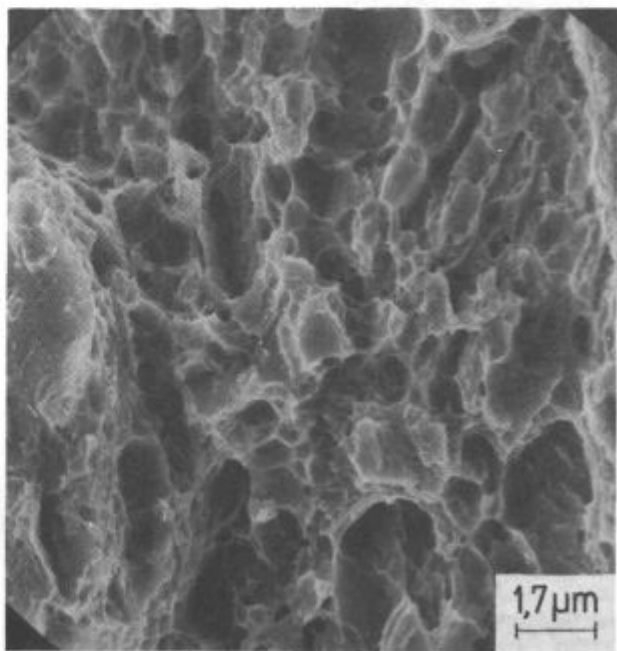
3.5 Micromorphology of Fractures

Microfractographic investigations of fracture surfaces of round notched tensile specimens charged with hydrogen were performed in a scanning electron microscope.

Fig. 7 shows a part of fracture surface of a round notched tensile specimen with fully martensitic tempered microstructure and with yield strength 1185 N mm^{-2} . Static load i.e. applied stress intensity factor $2190 \text{ N mm}^{-3/2}$ was close to the limiting value ($K_{TH} = 2180 \text{ N mm}^{-3/2}$) which caused the delayed fracture of the specimen after 181 hours. Right along the notch (above), an area of slow crack propagation can be seen separated by an unsharp boundary from the fracture surface formed by an instantaneous failure (below).

The area of slow crack propagation, which is completely undefined at low magnification, is shown in Fig. 8 at a higher magnification. This area is predominantly ductile and irregularly shaped dimples are found next to the well defined dimples. Irregular dimples indicate that decohesion occurred at a very low plastic deformation. It is also possible that some details are a consequence of cleavage too.

A similar micromorphology of the area of slow crack propagation is observed on samples with the tempered

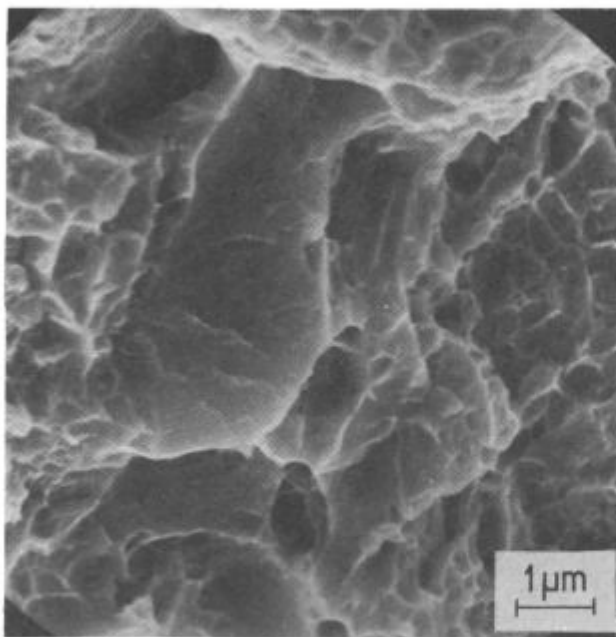


Slika 8

Področje počasne propagacije s slike 7. Pretežno duktilna oblika preloma.

Fig. 8

The area of slow crack propagation from Fig. 7. Predominantly ductile fracture.



Slika 9

Področje počasne propagacije na preizkušancu s popuščeno martenzitno mikrostrukturo ter mejo plastičnosti 1290 N mm^{-2} . Duktilna oblika preloma s posameznimi cepilnimi ploskvami.

Fig. 9

The area of slow crack propagation in specimen with the tempered martensitic microstructure and yield strength 1290 N mm^{-2} . Ductile fracture with single cleavage facets.

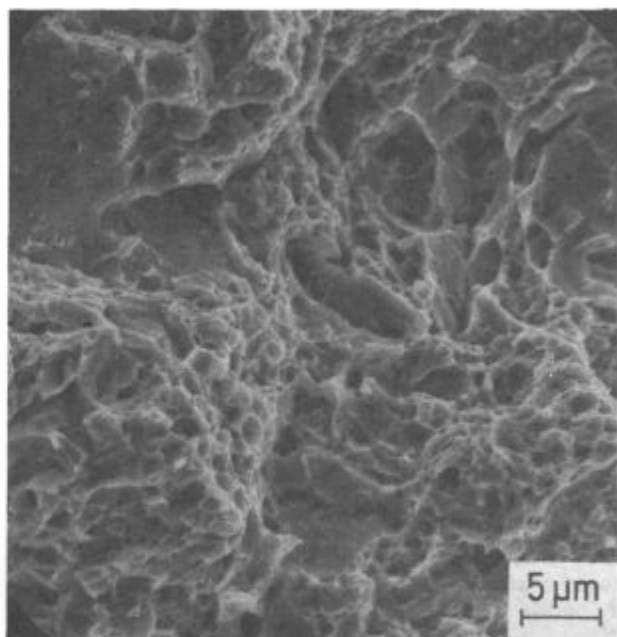
obremenitev, namreč aplicirani napetostni intenzitetni faktor $2190 \text{ Nmm}^{-3/2}$, je bila blizu mejni vrednosti ($K_{TH} = 2180 \text{ Nmm}^{-3/2}$), kar je povzročilo zapozneli lom preizkušanca po 181 urah.

Neposredno ob zarezi (zgoraj) je moč videti cono počasnega napredovanja mikrorazpok, ne ostro ločeno od prelomne površine, nastale s hipno porušitvijo (spodaj).

Cona počasnega napredovanja mikrorazpok, ki je pri nizki povečavi povsem neopredeljiva, je pri večji povečavi prikazana na sliki 8. To področje je pretežno duktilno, poleg dobro definiranih jamic pa najdemo tudi jamicice nepravilnih oblik. Nepravilne jamicice kažejo, da se je dekohezija izvršila z zelo malo plastične deformacije in prav mogoče je, da so nekateri detaili tudi proizvod cepljenja. Podobno mikromorfologijo preloma v coni počasnega napredovanja mikrorazpok zasledimo tudi na preizkušancih s popuščeno martenzitno-bainitno mikrostrukturo, medtem ko je na preizkušancih s popuščeno martenzitno mikrostrukturo ter mejo plastičnosti 1290 Nmm^{-2} že tudi občutnejši delež cepilnih ali kvazicepilnih ploskvic (slika 9). Področje naglo zlomljenega osrednjega dela preizkušanca s slike 7 je pri večji povečavi prikazano na sliki 10. Prevladujejo področja duktilnega tipa preloma, čeprav je opaziti tudi cepilne oziroma kvazicepilne ploskvice, a v manjšem obsegu.

Podobna je mikromorfologija preloma osrednjega, naglo zlomljenega dela preizkušancev s popuščeno martenzitno-bainitno mikrostrukturo, kot tudi preizkušancev s popuščeno martenzitno mikrostrukturo ter mejo plastičnosti 1290 Nmm^{-2} , čeprav je v slednjem primeru število kvazicepilnih ploskvic povečano.

Pojavljanje cepilnega oziroma kvazicepilnega tipa preloma v coni počasnega napredovanja mikrorazpok je le sporadično, v nasprotju s prevladajočo duktilno obliko preloma, zato sklepamo, da je nukleacija mikro-



Slika 10

Področje naglega loma iz slike 7. Duktilno, cepilno in kvazi-cepilno.

Fig. 10

Region of fast fracture from Fig. 7. Ductile, cleavage and quasi-cleavage.

martenitic-bainitic microstructure, while a noticeable amount of cleavage or quasi-cleavage facets appear in the samples with the martensitic microstructure and the yield strength 1290 N mm^{-2} (Fig. 9).

The area of fast fracture, already shown in Fig. 7, is shown again in Fig. 10 at a higher magnification. Here, the ductile type of fracture prevails though cleavage or quasi-cleavage facets can also be observed but in smaller extent.

A similar micromorphology of the areas of fast fracture is also observed on the samples with the tempered martensitic-bainitic microstructure as well as on the samples with the tempered martenitic microstructure and with yield strength 1290 N mm^{-2} , though in the latter case the number of quasi-cleavage facets is larger.

Cleavage or quasi-cleavage type of fracture in the area of slow crack propagation is merely sporadic in comparison to the prevailing ductile type of the fracture, thus the conclusion can be made that the crack nucleation as well as the slow crack propagation are mainly strain induced processes related to the decrease of fracture ductility i. e. decrease of the microplasticity in the area of stress induced segregation of hydrogen at the crack tip.

4. CONCLUSIONS

An appropriate method was developed for the detection of the nucleation and the propagation of microcracks at the notch tip of hydrogen charged static loaded cylindrical round notched tensile specimens. The limit of the detectability of microcrack propagation was about $0.1 \mu\text{m}$.

Measurements of the threshold stress intensity factor K_{TH} of the hydrogen charged chromium-molybdenum C.4732 steel with the tempered martensitic microstruc-

razpok ter njih počasno napredovanje deformacijsko inducirani proces povezan s poslabšanjem lomne duktilitnosti, t. j. poslabšanjem mikroplastičnosti v področju napetostno induciranega segregiranja vodika ob konici razpoke.

4. ZAKLJUČKI

V okviru opravljenega dela je bila razvita primerna metoda za preučevanje nastajanja ter napredovanja mikrorazpok iz korena zareze na obodu navodičenih ter statično obremenjenih cilindričnih nateznih preizkušancev z zarezo. Najmanjši korak propagacije mikrorazpok, ki ga je bilo moč zaslediti, je znašal okoli $0,1 \mu\text{m}$.

Merjenja mejnega napetostnega intenzitetnega faktorja K_{TH} navodilnega krom-molibdenskega jekla, vrste Č.4732, z mikrostrukturo popuščenega martenzitom oziroma popuščeno martenzitno-bainitno mikrostrukturo enake meje plastičnosti, kažejo, da majhne mikrostrukturne variacije preiskovanega jekla ne vplivajo na K_{TH} .

Ti rezultati se ujemajo z ugotovitvami Nakasata in Terasakija³², ki potrjujeta, da mejni napetostni intenzitetni faktor K_{Ic} pri enaki trdnosti jekla ni odvisen od mikrostrukturnih variacij visokotrdnega jekla. Če je ta ugotovitev splošna, potem je utemeljena hipoteza, po kateri je nukleacija mikrorazpok, ki povzroči zapozneli lom jekla, vedno omejena na martenzitne dele mikrostrukture (najprej dosežena $[H]^*$). Le na ta način namreč lahko razložimo, da majhni deleži bainita v pretežno martenzitni mikrostrukturi popuščenega visokotrdnega jekla nimajo vpliva na mejni napetostni intenzitetni faktor. Zdi se, da se različna jekla pri enaki vsebnosti vodika ter enaki meji plastičnosti v pogledu nukleacije mikrorazpok obnašajo kot elastični kontinuum.

Merjenja kritičnega napetostnega intenzitetnega faktorja kažejo, da majhne koncentracije vodika v preiskovanem jeklu nimajo opaznejšega vpliva na lomno žilavost jekla. Pač pa je pri enaki meji plastičnosti lomna žilavost (v nasprotju z mejnim napetostnim intenzitetnim faktorjem) odvisna tudi od majhnih mikrostrukturnih variacij jekla, saj ima jeklo s popuščeno martenzitno-bainitno mikrostrukturo nekoliko višjo lomno žilavost, kot isto jeklo s popuščeno martenzitno mikrostrukturo enake meji plastičnosti.

Rezultati teh preiskav se ujemajo s podatki, ki so jih objavili Ohtani, Terasaki in Kunitake³³, ki so povečano žilavost duplex mikrostrukture razlagali s koristno vlogo majhnih deležev bainita pri zmanjšanju delov posameznih avstenitnih zrn, ki se transformirajo v martenzit. Takšna mikrostruktura ima povečano odpornost proti napredovanju razpok, t. j. manjšo občutljivost k zapozneemu lomu.

Porajanje mikrorazpok v področju maksimalnih deformacij, kot tudi pretežno duktilna oblika preloma v coni počasnega napredovanja mikrorazpok navajata k sklepui, da je nukleacija mikrorazpok deformacijsko inducirani proces, povezan s poslabšanjem lomne duktilitnosti med trajanjem obremenjevanja.

ture or the tempered martensitic-bainitic microstructure and with the same yield strength showed that small microstructure variations of the investigated steel had no influence on K_{TH} .

These results confirm the Nakasato's and Terasaki's statements³² according to which the threshold stress intensity factor K_{Ic} at the same tensile strength does not depend on the microstructure variations of high strength steel. If this statement is general, the hypothesis suggesting that the microcrack nucleation leading to the delayed fracture is always confined to martensitic areas of the microstructure ($[H]^*$ is at first reached) has argument. It seems that this is the only way to explain the lack of influence of small portion of bainite in a predominantly martensitic microstructure of the tempered high strength steel on the threshold stress intensity factor. As far as the crack nucleation is concerned, it seems that various steels with the same yield strength and the same hydrogen concentration behave as an elastic continuum.

The measurements of the critical stress intensity factor show that small concentrations of hydrogen in the investigated steel has no noticeable influence on the fracture toughness of steel. However, at the same yield strength the fracture toughness (contrary to the threshold stress intensity factor) depends also on small microstructure variations of steel, since steel with the tempered martensitic-bainitic microstructure has slightly higher fracture toughness than the same steel with the tempered martensitic microstructure and with the same yield strength. The results of this investigation agree with the data published by Ohtani, Terasaki and Kunitake³³ who explained the higher toughness of the duplex microstructure by the beneficial effect of small quantity of bainite which reduces the size of single austenite-grain parts in which the martensitic transformation takes place. Such a microstructure has a better resistance to crack propagation i. e. it is less sensitive to the delayed fracture.

The nucleation of the crack in the region of maximal strain as well as the predominantly ductile type of fracture in that area suggest the conclusion that the nucleation of microcracks is a strain induced process related to the decrease of fracture ductility during the loading.

LITERATURA/REFERENCES

1. G. L. Hanna, A. R. Troiano in E. A. Steigerwald: Transactions of the ASM, 57, 1964, 658-671
2. A. R. Troiano: Transactions of the ASM, 52, 1960, 54
3. L. S. Darken in R. P. Smith: Corrosion 5, 1949, 1
4. R. A. Oriani: Acta Metall. 18, 1970, 147
5. Y. Sakamoto in J. Eguchi: Proc. Japan Congress on Materials Research 19, 1976, 91
6. A. P. Miodownik: Stress corrosion cracking and hydrogen embrittlement of iron base alloys, NACE, Huston, 1977
7. A. Zielinski, B. Lunarska in M. Smialowski: Acta Metall. 25, 1977, 551

8. A. J. Kumnick in H. H. Johnson: *Acta Metall.* 28, 1980, 33
9. A. M. Adair in R. E. Hook: *Acta Metall.* 10, 1962, 741
10. A. J. Kumnick in H. H. Johnson: *Metallurgical Transactions* 5A, 1974, 1199
11. G. M. Evans in E. C. Rollason: *Japan Iron Steel Inst.*, 1969, 1484
12. D. M. Allen-Booth in J. Hewitt: *Acta Metall.* 22, 1974, 171
13. H. Hargi, Y. Hayashi in L. L. Shreir: *Corrosion Science* 11, 1971, 25
14. G. W. Hong in J. Y. Lee: *J. Mat. Sci.* 18, 1983, 271
15. T. Asaoka, G. Lapasset in M. Aucouturier: *Corrosion* 34, 1978, 39
16. G. M. Pressouyre in I. M. Bernstein: *Metallurgical Transactions* 9A, 1978, 1571
17. A. McNabb in P. K. Foster: *Trans. Am. Inst. Min. Engrs.* 227, 1963, 618
18. W. Tyson: *Canadian Metallurgical Quarterly*, Vol. 18, 1979, 1—11
19. J. C. M. Li, L. S. Darken in R. A. Oriani: *Zeitschrift für Physikalische Chemie Neue Folge* 9, 1966, 271
20. H. L. Ewalds in R. J. H. Wanhill: *Fracture mechanics*, Edward Arnold Ltd., 1985
21. povzeto po A. G. Guy: *Essentials of Materials Science*, McGraw-Hill, 1976
22. W. W. Gerberich: Effect of hydrogen on high-strength and martensitic steels, *Hydrogen in Metals — Proceedings of an international conference*, 23.—27. September 1973, Seven Springs Conference Center, Champion, Pa. USA, Library of Congress Catalog Card Number: 73—86455
23. R. A. Oriani: *Ber. der Buns. Gesell.* 76, 1972, 848
24. C. D. Beachem: *Metallurgical Transactions* 3, 1972, 437
25. K. Farrell in A. G. Quarrell: *J. Iron Steel Inst.*, 202, 1964, 1002
26. C. D. Kim in A. W. Loginow: *Corrosion* 24, 1968, 313
27. K. Heckel: *Einführung in die technische Anwendung der Bruchmechanik*, Carl Hanser Verlag, München 1970
28. B. Moran in D. M. Noris: *Metallurgical Transactions A*, 1978, 1685
29. L. S. Darken in R. P. Smith: *Corrosion* 5, 1949, 60
30. B. Ule: *Zapozneli lom zaradi vodika v jeklu*, Magistrsko delo, Univerza E. Kardelja v Ljubljani, 1987
31. S. T. Rolfe in S. R. Novak: Slow-bend K_{Ic} testing of medium-strength high-toughness steels, *STP 463*, 1970, 124—159 kot tudi R. B. Scarlin in M. Shakeshaft: *Metals Technology*, Jan. 1981, 1—9
32. F. Nakasato in E. Terasaki: *Transactions ISIJ*, 15, 1975, 290—291
33. H. Ohtani, F. Terasaki in T. Kunitake: *Transactions ISIJ*, 12, 1972, 185